Self-Consistent-Field and Hybrid Particle-Field Theory Simulation of Confined Copolymer and Nanoparticle Mixtures

Qiangyong Pan, Chaohui Tong, and Yuejin Zhu*

Department of Physics, Ningbo University, Ningbo 315211, China

ABSTRACT In this paper, we used combined self-consistent-field and hybrid particle-field theory to explore the self-assembly behavior of diblock copolymer—nanoparticle mixtures confined between two concentric circular walls. The simulation reveals that the structural frustration, the loss of conformational entropy of the copolymer, and the radii of the two concentric circles have great influence on the morphologies of the system. We also discusss the underlying mechanism of controlling the self-assembly of such a system in terms of enthalpic interaction between particles and copolymers, steric repulsive interactions between particles, and the conformational entropy of copolymers, and a representative phase diagram in terms of block ratio and the particle volume fraction is constructed. This study suggests a route to help experimentalists better create high-performance nanodevices.

KEYWORDS: self-assembly · diblock copolymer · nanoparticle · confinement effects · self-consistent field theory · hybrid particle-field theory

The morphologies associated with the self-assembly of diblock copolymer—nanoparticle have attracted tremendous academic and industrial interests in recent years.[1−7] Because the block copolymers are composed of two kinds of different segments, it can be used as a template for the self-assembly of nanoparticles by controlling the corresponding volume fraction, molecular weight, and the interaction between the two distinct polymer blocks.[8] From the perspective of the theory and application, diblock copolymer—nanoparticle mixtures are also very interesting because they can form ordered phase structure with 10—100 nm characteristic scale. However, this can hardly be achieved by the traditional sophisticated top-down technology.[9−11]

In the bulk, the diblock copolymer—nanoparticle mixtures can form abundant phase structures such as lamellae, hexagonally packed cylinders, helices, and toroids, *etc.* However, there often exist some defects in these structural phases, thus limiting the application of these structures in some sophisticated devices. Some additional fields such as flow fields, electric fields, or magnetic fields can be incorporated into the system in order to preserve the long-range order in phase structures and reduce the negative effect of the defects.[12−15] In addition, when the diblock copolymer—nanoparticle mixtures are confined in a physical environment, unusual morphologies not accessible in the bulk would emerge, thus offering new opportunities to create novel nanostructures for industrial applications.[16−23] Balazs *et al.* reported the self-assembly of diblock copolymer—nanoparticle mixtures confined between two parallel surfaces and observed stripes oriented either parallel or perpendicular to the walls at different conditions.[24,25] In our previous work, we also have systematically studied the phase behaviors of diblock copolymer—nanoparticle mixtures under nanonopore confinment, and discovered a series of interesting phase structures.[26] So far, the studies of the self-assembly of diblock copolymer—nanoparticle mixtures confined between two concentric circular walls has not been investigated. Recently, Fredrickson *et al.*[27] developed a hybrid particle-field (HPF) simulation technique for polymeric fluids with embedded particles. The particle coordinates are explicitly retained as degrees of freedom. This HPF description is reminiscent of the Car—Parrinello technique for conducting *ab initio* molecular dynamics.[28] In these studies, the method of combined self-consistent field theory (SCFT) for dicopolymer and the density functional theory for particles (DFT) has been used for studying the self-assembly and morphologies of these systems.[1,29] This method has

*Address correspondence to zhuyuejin@nbu.edu.cn.

Received for review August 2, 2010 and accepted December 10, 2010.

Published online December 20, 2010. 10.1021/nn101886x

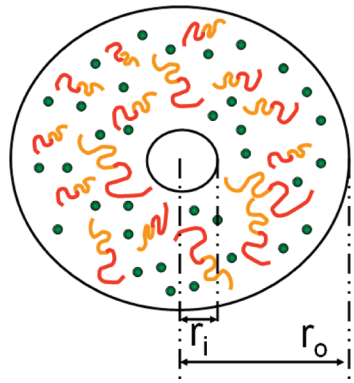

Figure 1. Schematic representation of the system. The red lines, orange lines, and circles filled with green color denote block A, block B, and nanoparticles, respectively. The radius of inner and outer ring is r_i and r_o.

the advantage of requiring no prior knowledge of the equilibrium structure of the system. However, it is not very precise in describing the particles, because DFT only provides the distributions of particles and particle centers without more detailed information of particles such as their coordinates.

In this paper, we study the self-assembly and phase behaviors of diblock copolymer−nanoparticle mixtures confined between two concentric circles using the combined self-consistent-field and hybrid particle-field theory (SCFT/HPF). HPF offers information including the particles' coordinates which show a good agreement to the experimental results.

RESULTS AND DISCUSSION

In the present work, we consider a system with volume V, containing n_D AB diblock copolymers, and n_P nanoparticles, confined between two concentric circles (Figure 1). The volume fractions of the copolymer and particles are ϕ_D and $1 - \phi_D$, respectively. All the diblock copolymer chains are flexible. Each copolymer chain is composed of total N segments of a statistical length a, the block composition is f (Nf segments of A per chain).

It is assumed that the particles are chemically identical to block A, setting $\chi_{AP}N = 0.0$ and $\chi_{BP}N = \chi_{AB}N = 20.0$. Thus the particles will be preferentially localized in the A domains. The wall is attractive to the block B with $V_{OB} = -0.3$, and repulsive to block A with $V_{OA} = 0.3$. Furthermore, the chain length of the diblock copolymer is set to be 100, while the particle size is fixed at $R_P = 0.2R_g$. The block copolymer is asymmetric with block A fraction of 0.28.

The equilibrium morphology of such a composite system is changed with the increase of ϕ_p, as shown in Figure 2, and the particles' positions are also obtained simultaneously, as shown in Figure 3. As can be seen from Figure 2a,c, with the increase of the particle concentration ϕ_p, there is a phase transition from the cylinders (C) phase to the concentric lamellar rings (L) phase, which is in good agreement with the experimental results.[27] The phase transition is vividly illustrated in the

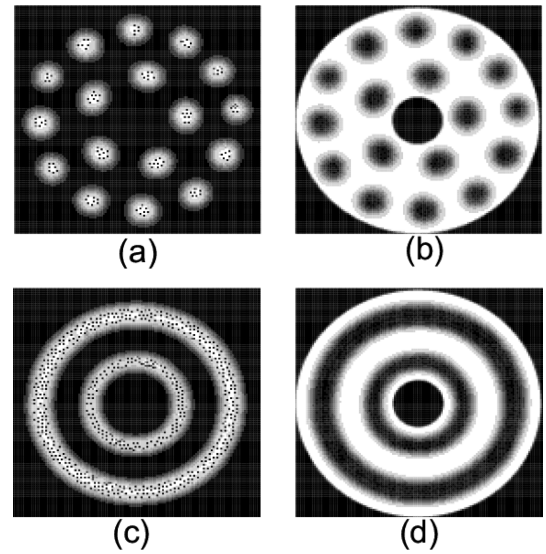

Figure 2. Density distributions of the diblock copolymer under a two-concentric circular wall confinement with a block ratio $f = 0.28$, $r_i = 1.2R_g$, $r_o = 6.4R_g$. (a,b) $\phi_p = 0.02$; (c,d) $\phi_p = 0.19$. Plots on the left represent the distribution of block A, and plots on the right represent the distribution of block B. Light regions indicate high densities, while dark regions indicate low densities.

schematic representations shown in Figure 4. This morphological transition results from the competition among the enthalpic interactions between particles and polymers and the steric effect due to the excluded volume interaction between particles. When the particle concentration ϕ_p is low, the block copolymer component is in majority. So the enthalpic interaction between particles and polymers plays a dominant role in forming the cylinders phase. With the enhancement of particle concentration, the steric repulsive interactions between particles become stronger, leading to the decrease of the conformational entropy of the copolymers. To compensate for the conformational entropy of copolymers, concentric lamellar rings phase forms. Figure 5 shows the average entropy of a single chain and the average steric repulsive interaction of a single particle with the increase of the particle concentration. From Figure 5a, it can be seen that the average entropy of a single chain decreases with the increase of particle concentration. The decrease of the average en-

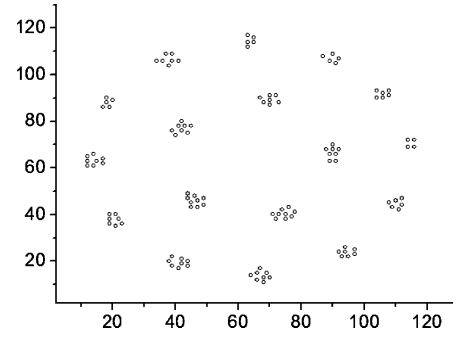

Figure 3. The particles' positions in the two-dimensional coordinate corresponding to Figure 2a are displayed; small circles represent particles.

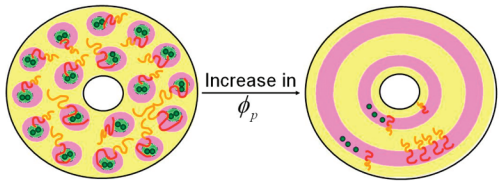

Figure 4. Schematic representations of the cylinders (C) phase (on the left) and concentric lamellar rings (L) phase (on the right), corresponding to Figure 2.

tropy of a single chain is most pronounced from 0.02 to 0.18. With the further increase of the particle concentration, the profile of the average entropy of a single chain begins to level off. Meanwhile, Figure 5b reflects the change of average steric repulsive interaction of a single particle with the particle concentration. Similarly, Figure 6 illustrates the equilibrium morphology of such a system with a block ratio $f = 0.55$. With the increase of the particle concentration ϕ_p, a phase transition from the concentric lamellar rings (L) phase to the cylinders (C) phase takes place. Correspondingly, the concentric lamellar rings (L) phase, cylinders (C) phase are schematized in Figure 7. Such a phase transition induced by the conformational entropy of copolymers is also observed by Balazs *et al.*[1,29] in their study of the self-assembly of block copolymer and particles. From both Figures 2 and 6 it can be clearly seen that particles are more or less uniformly distributed inside the block *A* domain.

To study the effects of block ratio *f* and the particle concentration on the self-assembled structures of the composite system, the phase diagram of such a composite system in terms of block ratio and the particle concentration is obtained at radii of inner and outer rings $r_i = 1.2R_g$, $r_o = 6.4R_g$, as shown in Figure 8.

As shown in Figure 8, when the particle concentration ϕ_p is relatively low and the block ratio *f* is small, cylinders rich in block A with the particles embedded are distributed nonhexagonally in block B domain, different from the morphology in the bulk. Although the mixtures thermodynamically prefer to form the hexagonal cylinders phase, the structure frustration introduced by confining walls leads to nonhexagonal packing of cylinders. As block ratio *f* approaches the symmetric point of 0.5, a concentric lamellar rings phase naturally appears. On the other hand, when block B is in minority,

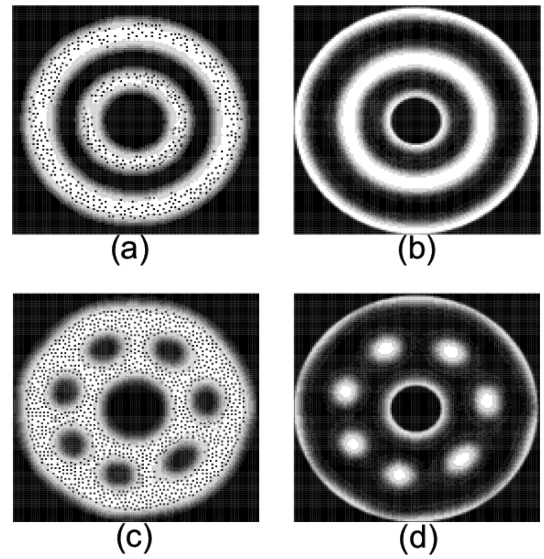

Figure 6. Density distributions of the diblock copolymer under two concentric circular wall confinement with a block ratio $f = 0.55$, $r_i = 1.2R_g$, $r_o = 6.4R_g$. (a,b) $\phi_p = 0.06$; (c,d) $\phi_p = 0.23$. Plots on the left represent the distribution of block A, and plots on the right represent the distribution of block B. Light regions indicate high densities, while dark regions indicate low densities.

the block B domain exhibits a nonhexagonal cylinder pattern. However, the cylinder phase is not symmetric to the previous nonhexagonal structure of A, because block B is attracted to walls in order to reduce the interfacial energy. From the phase diagram we can also see there exists an intermediate CL phase, which contains both cylinders and concentric lamellar rings. It would be very interesting to compare the phase diagram of the diblock copolymer/particle mixtures in the confined environment studied here with that in the bulk. Using Monte Carlo simulation in three-dimensional space, Huh *et al.* constructed the phase diagram of a diblock copolymer/particle mixture in the bulk in terms of the block ratio and the particle volume fraction.[30] A common feature in the phase diagram shown in Figure 8, and that shown in Figure 3 in ref 30, is that the phase boundary lines curve leftwards. This is because particles are preferentially attracted to block A. With the increase of the volume fraction of particles at a fixed block ratio, the total volume fraction of particles and block A increases accordingly. Nonetheless, due to the

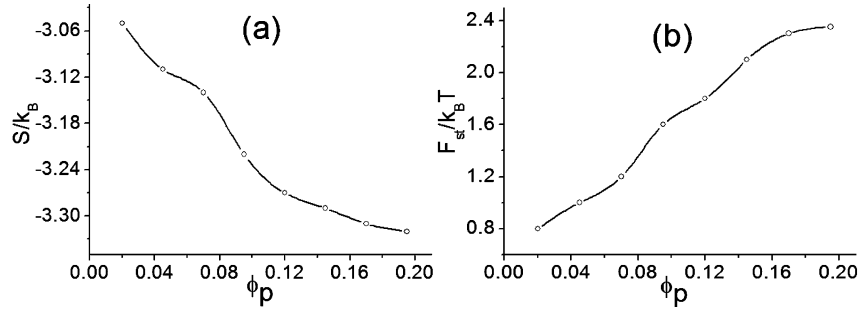

Figure 5. (a) Average entropy of single chain S/k_B, (b) average steric repulsive interaction of single particle F_{st}/k_BT, as a function of particle concentration ϕ_p.

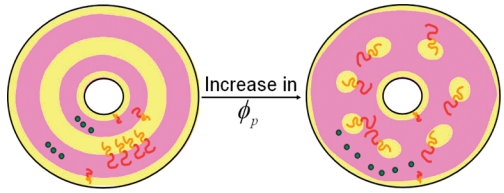

Figure 7. Schematic representations of the concentric lamellar rings (L) phase (on the left) and cylinders (C) phase (on the right), corresponding to Figure 6.

physical confinement, the phase behaviors of the composite in the present study display some unique features. As shown in Figure 8, there is a new phase dubbed CL which is absent in the bulk. Furthermore, there are some structural differences in the cylindrical and lamellar phases between the bulk and the confined nanocomposites. As pointed out already, in the cylindrical phase, due to the physical confinement and the incommensurate characteristics between the domain size in the bulk and the physical size of the confining environment, the cylinders are not hexagonally uniformly distributed. For the lamellar phase of the nanocomposite confined between two concentric walls, due to the attractive interaction between the wall and the block B, the single layer of block B segments wet the two walls; in between, double layers of block B segments form the concentric lamellar ring, resulting in the doubling of its width compared to the single layers near the two walls. These single and double layers of block B segments forming the concentric lamellar phase can be clearly identified in Figure 2d and Figure 6b. Besides the concentric lamellar phase, when the separation between the inner and the outer walls is comparable to the size of the block copolymer, a new perpendicular lamellar phase emerges, as shown in Figure 9e, which will be discussed later on. This perpendicular lamellar phase is not accessible in the bulk.

In the system of copolymer−nanoparticle mixtures confined in the nanopore, the radius of the confining pore has a significant effect on the phase behaviors of the mixtures.[26] We vary the radii of two concentric rings to explore the equilibrium morphologies of composites. Here, the radius of outer ring is fixed, the radius of inner ring is varied. As the radius of inner ring increases, the morphologies of the composite change dramatically due to the stronger physical confinement of two walls, especially when the copolymer is asymmetric. If the copolymer is symmetric, the morphology of the mixtures remains the concentric lamellar rings phase with the increase of the radius of inner ring such as Figure 9c,d. On the other hand, if the copolymer is asymmetric, the block A domains become a disorder state first, which then turns to the cylinders (C) phase again until the separation ($D = r_o - r_i$) between two concentric rings is comparable to the characteristic period of the copolymer domains as shown Figure 6a,b.

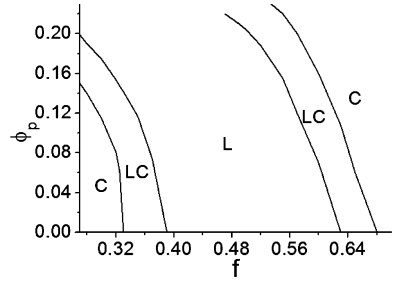

Figure 8. Phase diagram for diblock copolymer−nanoparticle mixtures confined between two concentric circular walls with different block ratio f and particle concentration ϕ_p at radii of inner and outer rings $r_i = 1.2R_g$, $r_o = 6.4R_g$. Where C denotes the cylinders phase, L denotes the concentric lamellar rings phase, while the CL phase contains both cylinders and concentric lamellar rings.

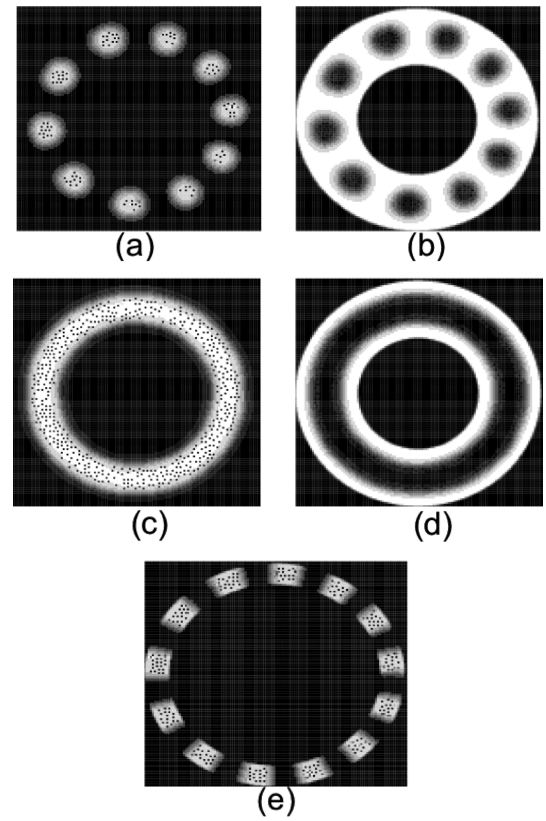

Figure 9. Typical monomer density distributions for the cylinders (C) phase, concentric lamellar rings (L) phase, and perpendicular lamellar ($L_\perp$) phase that form in the two concentric rings. (a,b) $f = 0.28$, $\phi_p = 0.02$, $r_i = 3.0R_g$, $r_o = 6.4R_g$; (c,d) $f = 0.5$, $\phi_p = 0.05$, $r_i = 3.0R_g$, $r_o = 6.4R_g$; (e) $f = 0.5$, $\phi_p = 0.05$, $r_i = 5.0R_g$, $r_o = 6.4R_g$.

However, the perpendicular lamellar ($L_\perp$) phase emerges if separation ($D = r_o - r_i$) is small enough, as shown is Figure 9e. This is because when D is sufficiently small, the two concentric circular walls could approximately serve essentially as two parallel walls. Balazs *et al.* reported the self-assembly of diblock copolymer−nanoparticle mixtures confined between parallel walls, with stripes oriented either parallel or perpendicular to the walls with different distance between the two walls.[24,25] In this article, although the walls have a weak preferential interaction with one of the blocks, the equilibrium structure of the system is the

perpendicular lamellar ($L_\perp$) phase when D is less than the characteristic period of the copolymer domains, so the structural frustration can be released.

CONCLUSIONS

We have applied the combined self-consistent-field and hybrid particle-field theory (SCFT/HPF) to investigate the behavior of diblock copolymer−nanoparticle mixtures confined between two concentric walls. Our studies show that particles have a great influence on the morphologies of the system. It is observed that the increase of the particle concentration can promote the phase transition from the cylinders (C) phase to the concentric lamellar rings (L) phase or from the concentric lamellar rings (L) phase to the cylinders (C) phase, respectively. And we obtain not only many new structrues but also the particles' coordinates, which is consistent with a series of experimental results. We also analyze the effects of the enthalpic interaction between particles and polymers, steric repulsive interactions between particles, and conformational entropy of copolymers in determining the equilibrium structures. A corresponding phase diagram is constructed. The effect of confinement on morphologies of the system is studied. When the separation (D) between the two concentric walls is sufficiently small, the two walls essentially serve as two parallel walls. So the perpendicular lamellar ($L_\perp$) phase emerges when the copolymer is symmetric. Our results reveal a new mechanism to stabilize the orderings of diblock copolymer−nanoparticle mixtures confined in a two concentric ring walls and could provide useful guidance for experimental designs.

METHODS

In the framework of the SCFT/HPF theory, we assume that the mixtures are incompressible, with each polymer segment occupying a fixed volume ρ_0^{-1}. The incompressibility constraint is taken to be $\varphi_A(\vec{r}) + \varphi_B(\vec{r}) + \varphi_P(\vec{r}) = \Phi_O(\vec{r})$, and the incompressibility condition is enforced as follows:[25]

$$\begin{aligned}\Phi_0(\vec{r}) &= \left[1 - \cos\left(\frac{\pi(r_o - r)}{\varepsilon}\right)\right]/2 && \text{(if } r \text{ is on the outer boundary of the ring)}\\ &= 1 && \text{(if } r \text{ is in the ring)}\\ &= \left[1 - \cos\left(\frac{\pi(r - r_i)}{\varepsilon}\right)\right]/2 && \text{(if } r \text{ is in the ring)}\end{aligned} \tag{1}$$

where ε is taken such that $\varepsilon < R_g$. In this paper, we choose $\varepsilon = 0.2R_g$. The local volume fraction of particles is $\varphi_P(\vec{r}) = \sum_j^{n_p} {}_1h(\vec{r} - \vec{r}_j)$ where[27]

$$\begin{aligned}h(\vec{r} - \vec{r}_j) &= 1 && \text{(if } r \text{ is in particle } j)\\ &= \left[1 + \cos\left(\frac{\pi|r - r_j|}{\Delta}\right)\right]/2 && \text{(if } r \text{ is on the boundary of particle } j)\\ &= 0 && \text{(if } r \text{ is not in particle } j)\end{aligned} \tag{2}$$

and the width of boundary of each particle is taken to be $\Delta = 0.04R_g$. The interaction field between either the particles or the copolymers with the confining wall is described by $H_i(\vec{r})$, which has the following mathematic expression:[31]

$$\begin{aligned}\frac{H_i(\vec{r})}{\chi N} &= \infty && \text{(if } r \text{ is not in the the ring)}\\ &= V_O\{\exp[(r - r_o + \delta + \varepsilon)/\lambda] - 1\} && \text{(if } r \text{ is on the outer boundary of the ring)}\\ &= V_O\{\exp[(r_i - r + \delta + \varepsilon)/\lambda] - 1\} && \text{(if } r \text{ is on the inner boundary of the ring)}\\ &= 0 && \text{(if } r \text{ is in the ring)}\end{aligned} \tag{3}$$

where V_O denotes the strength of the surface field, the cutoff length δ and the decay length λ of the surface interaction are the same as those in ref 26.

Using the combined self-consistent-field and hybrid particle-field theory (SCFT/HPF),[29,32] the dimensionless free energy F can be obtained as

$$\begin{aligned}\frac{NF}{\rho_0 K_B T V} = -\phi_D \ln\left(\frac{Q_D}{V\phi_D}\right) + \frac{1}{V}\int d\vec{r}\,[&\chi_{AB}N\varphi_A(\vec{r})\varphi_B(\vec{r}) + \chi_{AP}N\varphi_A(\vec{r})\varphi_P(\vec{r}) + \chi_{BP}N\varphi_B(\vec{r})\varphi_P(\vec{r}) - W_A(\vec{r})\varphi_A(\vec{r}) - W_B(\vec{r})\varphi_B(\vec{r}) +\\ &H_A(\vec{r})\varphi_A(\vec{r}) + H_B(\vec{r})\varphi_B(\vec{r}) + H_P(\vec{r})\varphi_P(\vec{r}) - \xi(\vec{r})(1 - \varphi_A(\vec{r}) - \varphi_B(\vec{r}) - \varphi_P(\vec{r}))]\end{aligned} \tag{4}$$

where K_B is the Boltzmann constant and T is the absolute temprature; $\chi_{\mu\upsilon}$ characterize the Flory−Huggins interaction parameter between species μ and υ; $\varphi_u(\vec{r})$ expresses the local volume fraction of each constituent of the mixtures. The pair interactions between different constituents of the mixtures are determined by a set of effective chemical potential fields $W_u(\vec{r})$ (u = A,B,P), replacing the actual interactions in the system. $\xi(\vec{r})$ is the Lagrange multiplier which enforces the incompressibility condition of the system; Q_D is the partition function of one copolymer chain, and it is given by

$$Q_D = \int d\vec{r}\, q(\vec{r}, s)\, q^+(\vec{r}, s) \tag{5}$$

Minimizing the free energy in eq 4 with respect to the local volume fractions and their conjugate fields as well as the Lagrange multiplier, the following self-consistent equations describing the equilibrium morphologies of the system can be obtained:

$$W_A(\vec{r}) = \chi_{AB}N\varphi_B + \chi_{AP}N\varphi_P + H_A(r) + \xi(\vec{r}) \tag{6}$$

$$W_B(\vec{r}) = \chi_{AB}N\varphi_A + \chi_{BP}N\varphi_P + H_B(r) + \xi(\vec{r}) \tag{7}$$

$$\varphi_A(\vec{r}) = \frac{\phi_D V}{Q_D}\int_0^f ds\, q(\vec{r}, s)\, q^+(\vec{r}, s) \tag{8}$$

$$\varphi_B(\vec{r}) = \frac{\phi_D V}{Q_D}\int_f^1 ds\, q(\vec{r}, s)\, q^+(\vec{r}, s) \tag{9}$$

$$\varphi_A(\vec{r}) + \varphi_B(\vec{r}) + \varphi_P(\vec{r}) = \Phi_O(\vec{r}) \tag{10}$$

In eqs 5, 8, and 9, $q(\vec{r},s)$ and $q^+(\vec{r},s)$ are the probabilities of finding the segment s at the position $\vec{r}$ with either end of the diblock copolymer chain free, and they satisfy the following modified diffusion equations

$$\frac{\partial q(\vec{r}, s)}{\partial s} = \nabla^2 q(\vec{r}, s) - W(\vec{r})\, q(\vec{r}, s) \tag{11}$$

$$\frac{\partial q^+(\vec{r}, s)}{\partial s} = -\nabla^2 q^+(\vec{r}, s) + W(\vec{r})\, q^+(\vec{r}, s) \tag{12}$$

where $W(\vec{r}) = W_A(\vec{r})$when $0 \le s \le f$, and $W(\vec{r}) = W_B(\vec{r})$ when $f < s \le 1$, with the initial conditions of $q(\vec{r},0) = 1$ and $q^+(\vec{r},1) = 1$, respectively.

The force on particle j can be written

$$T_j = -\frac{\partial(NF/\rho_0 K_B TV)}{\partial \vec{r}_j} \quad (13)$$

Then we can update corresponding position of the particle j with hybrid particle−field theory (HPF) by

$$\Delta\vec{r}_j = \gamma\vec{T}_j + \vec{R}_j \quad (14)$$

where $\vec{R}_j$ is a Gaussian random variable. We set $\vec{R}_j = 0$ and $\gamma = 0.2R_g^2$ for simplicity here.

The above self-consistent field equations (eqs 6−10) are numerically solved in the real-space, and it is assumed that the equilibrium is reached when the relative change in the free energy between two consecutive iteration steps is smaller than 10^{-6} (namely $\Delta F < 10^{-6}$), also the incompressibility condition is satisfied (namely $((\Phi_O(\vec{r})) - \varphi_A(\vec{r}) - \varphi_B(\vec{r}) - \varphi_P(\vec{r}))^{2)1/2} < 10^{-4}$). So we take the equilibrium phase to be the structure which has the lowest free energy. In the simulations, the sizes of the computational domain are 128 × 128 with periodic boundary conditions. It is noted that the resulting aggregate morphologies depend on the amplitude of the initial density fluctuations. The different initial density fluctuations result in different microstructures. So we use the same initial density fluctuation amplitude in all the simulations. Also, the simulations are repeated 8−10 times for different initial random states and different random numbers to ensure that the phenomena is not accidental.

Acknowledgment. The authors acknowledge financial support from the National Natural Science Foundation of China (Grant No. 10774079, 20954001, 21074062) and Natural Science Foundation of Zhejiang Province (Grant No. Y4090429). The Natural Science Foundation of Ningbo City (Grant No. 2009A610056) and K. C. Wong Magna Fund in Ningbo University are also acknowledged.

REFERENCES AND NOTES

1. Thompson, R. B.; Ginzburg, V. V.; Matsen, M. W.; Balazs, A. C. Predicting the Mesophases of Copolymer−Nanoparticle Composites. *Science* **2001**, *292*, 2469–2472.
2. Kim, B. J.; Fredrickson, G. H.; Hawker, C. J.; Kramer, E. J. Nanoparticle Surfactants as a Route to Bicontinuous Block Copolymer Morphologies. *Langmuir* **2007**, *23*, 7804–7809.
3. Birnkrant, M. J.; Li, C. Y.; Natarajan, L. V.; Tondiglia, V. P.; Sutherland, R. L.; Lloyd, P. F.; Bunning, T. J. Layer-in-Layer Hierarchical Nanostructures Fabricated by Combining Holographic Polymerization and Block Copolymer Self-Assembly. *Nano Lett.* **2007**, *7*, 3128–3133.
4. Chiu, J. J.; Kim, B. J.; Yi, G. R.; Bang, J.; Kramer, E. J.; Pine, D. J. Distribution of Nanoparticles in Lamellar Domains of Block Copolymers. *Macromolecules* **2007**, *40*, 3361–3365.
5. Matsen, M. W.; Thompson, R. B. Particle Distributions in a Block Copolymer Nanocomposite. *Macromolecules* **2008**, *41*, 1853–1860.
6. Vaia, R.; Baur, J. Materials Science: Adaptive Composites. *Science* **2008**, *319*, 420–421.
7. Zhang, L. S.; Lin, J. P. Hierarchically Ordered Nanocomposites Self-Assembled from Linear-Alternating Block Copolymer/Nanoparticle Mixture. *Macromolecules* **2009**, *42*, 1410–1414.
8. Bucknall, D. G.; Anderson, H. L. Polymers Get Organized. *Science* **2003**, *302*, 1904–1905.
9. Fredrickson, G. H.; Bates, F. S. Dynamics of Block Copolymers: Theory and Experiment. *Annu. Rev. Mater. Sci.* **1996**, *26*, 501–550.
10. Förster, S.; Plantenberg, T. From Self-Organizing Polymers to Nanohybrid and Biomaterials. *Angew. Chem., Int. Ed.* **2002**, *41*, 689–714.
11. Park, C.; Yoon, J.; Thomas, E. L. Erratum: Enabling Nanotechnology with Self Assembled Block Copolymer Patterns. *Polymer* **2003**, *44*, 6725–6760.
12. Chen, Z.; Kornfield, J. A.; Smith, S. D.; Grothaus, J. T.; Satkowski, M. M. Pathways to Macroscale Order in Nanostructured Block Copolymers. *Science* **1997**, *277*, 1248–1253.
13. Tong, C. H. The Finite Size Effect of Monomer Units on the Electrostatics of Polyelectrolyte Solutions. *J. Chem. Phys.* **2010**, *132*, 074904-1–074904-11.
14. Matsen, M. W. Electric Field Alignment in Thin Films of Cylinder-Forming Diblock Copolymer. *Macromolecules* **2006**, *39*, 5512–5520.
15. Thurn-Albrecht, T.; Schotter, J.; Kastle, G. A.; Emley, N.; Shibauchi, T.; Krusin-Elbaum, L.; Guarini, K.; Black, C. T.; Tuominen, M. T.; Russell, T. P. Ultrahigh-Density Nanowire Arrays Grown in Self-Assembled Diblock Copolymer Templates. *Science* **2000**, *290*, 2126–2129.
16. Warren, S. C.; Disalvo, F. J.; Wiesner, U. Erratum: Nanoparticle-Tuned Assembly and Disassembly of Mesostructured Silica Hybrid. *Nat. Mater.* **2007**, *6*, 156–161.
17. Stamm, M.; Sommer, J.-U. Polymer−Nanoparticle Films: Entropy and Enthalpy at Play. *Nat. Mater.* **2007**, *6*, 260–261.
18. Krishnan, R. S.; Mackay, M. E.; Duxbury, P. M.; Pastor, A.; Hawker, C. J.; Van Horn, B.; Asokan, S.; Wong, M. S. Self-Assembled Multilayers of Nanocomponents. *Nano Lett.* **2007**, *7*, 484–489.
19. Kang, Y.; Taton, T. A. Core/Shell Gold Nanoparticles by Self-Assembly and Crosslinking of Micellar, Block-Copolymer Shells. *Angew. Chem., Int. Ed.* **2005**, *44*, 409–412.
20. Kim, B.-S.; Taton, T. A. Multicomponent Nanoparticles *via* Self-Assembly with Cross-Linked Block Copolymer Surfactants. *Langmuir* **2007**, *23*, 2198–2202.
21. Ren, C.-L.; Ma, Y.-Q. Phase Behavior in Thin Films of Confined Colloid−Polymer Mixtures. *J. Am. Chem. Soc.* **2006**, *128*, 2733–2737.
22. Zhou, L.; Ma, Y.-Q. Phase Behavior of Nanoparticle−Copolymer Films Confined Between Polymer-Grafted Surfaces. *J. Phys.: Condens. Matter* **2008**, *20*, 095006-1–095006-5.
23. Ma, M. L.; Thomas, E. L.; Rutledge, G. C.; Yu, B.; Li, B. H.; Jin, Q. H.; Ding, D. T. Gyroid-Forming Diblock Copolymers Confined in Cylindrical Geometry: A case of Extreme Makeover for Domain Morphology. *Macromolecules* **2010**, *43*, 3061–3071.
24. Lee, J. Y.; Shou, Z. Y.; Balazs, A. C. Predicting the Morphologies of Confined Copolymer/Nanoparticle Mixtures. *Macromolecules* **2003**, *36*, 7730–7739.
25. Lee, J. Y.; Shou, Z. Y.; Balazs, A. C. Modeling the Self-Assembly of Copolymer−Nanoparticle Mixtures Confined between Solid Surfaces. *Phys. Rev. Lett.* **2003**, *91*, 1361031–1361034.
26. Yang, Q. H.; Li, M.; Tong, C. H.; Zhu, Y. J. Phase Behaviors of Diblock Copolymer−Nanoparticle Films under Nanopore Confinement. *J. Chem. Phys.* **2009**, *130*, 094903-1–094903-7.
27. Sides, S. W.; Kim, B. J.; Kramer, E. J.; Fredrickson, G. H. Hybrid Particle-Field Simulations of Polymer Nanocomposites. *Phys. Rev. Lett.* **2006**, *96*, 250601-1–250601-4.
28. Car, R.; Parrinello, M. Unified Approach for Molecular Dynamics and Density-Functional Theory. *Phys. Rev. Lett.* **1985**, *55*, 2471–2474.
29. Thompson, R. B.; Ginzburg, V. V.; Matsen, M. W.; Balazs, A. C. Block Copolymer-Directed Assembly of Nanoparticles: Forming Mesoscopically Ordered Hybrid Materials. *Macromolecules* **2002**, *35*, 1060–1071.
30. Huh, J.; Ginzburg, V. V.; Balazs, A. C. Thermodynamic Behavior of Particle/Diblock Copolymer Mixtures: Simulation and Theory. *Macromolecules* **2000**, *33*, 8085–8096.
31. Li, W.; Wickham, R. A.; Garbary, R. A. Phase Diagram for a Diblock Copolymer Melt under Cylindrical Confinement. *Macromolecules* **2006**, *39*, 806–811.
32. Tang, Q. Y.; Ma, Y. Q. Self-Assembly of Rod-Shaped Particles in Diblock-Copolymer Templates. *J. Phys. Chem. B* **2009**, *113*, 10117–10121.